Finite element analyses on a small masonry house prototype retrofitted using frp strips

Ahmad Basshofi Habieb[a*], Marco Valente[b], Gabriele Milani[b]

***Abstract**: This study presents a series of finite element analyses on the prototype of masonry house retrofitted using FRP strips. The model of the masonry house refers to the prototype scaled to 1:3 tested in an experimental campaign. The non-linear behavior of masonry is modeled through the Concrete Damage Plasticity (CDP) model, while the FRP and adhesive are modeled as two separated isotropic solid materials with elastic-plastic behavior. A good agreement between experimental and numerical result is obtained, indicating the increase of bearing capacity of the reinforced masonry prototype.*

Keywords: *finite element analysis, masonry house, FRP reinforcement, concrete damage plasticity, adhesive.*

INTRODUCTION

Masonry constructions are widely applied particularly in developing regions due to the economical reason. However, it is well known that masonry structures in general have very low seismic resistance because the shear resistance relies only on the shear capacity of the mortar joint between laying bricks. Retrofitting using fiber materials such as FRP or FRCM is considered as an economic and easy technical solution to improve the seismic capacity of masonry structures. In addition to suitable tensile strength, FRPs have no risk of corrosion after long term use so that they can be widely applied in various environment conditions with excellent durability. Researchers in [1] investigate the effectiveness of FRP strips reinforcement on three masonry churches located in Emilia Romagna region, Italy. The application of FRP materials is found very effective in increasing the masonry wall strength and displacement capacity both in shear and bending conditions. The stiffness of the retrofitted churches is not affected by the FRP application so that the seismic force demand can be maintained. In [2], a strengthening method using FRP and FRCM is proposed to restore the walls and vaults of St. Ann's Church in Zabkowice Slaskie, Poland as a solution to the cracking observed. The method involves injections into fissures and cracks, applying steel rods, strengthening rib elements with carbon FRP and consolidating the surface of the vault using carbon FRCM grids. The main advantages of the proposed intervention include fire resistance and resistance to corrosion.

The application of FRP reinforcement on a medieval bell tower in Serra San Quirico Italy is reported in [3]. An FRP tie system is applied to the inner walls and anchored at the base by a reinforced concrete slab, independent of the tower's foundation. Considering the probabilistic seismic hazard at the site, this intervention enhances the seismic capacity of the structure. Researchers in [4] propose the retrofitting of a masonry bell tower of Santa Maria del Carmine in Napoly, Italy, using glass FRP ties. An innovative solution has been applied by installing tie rods made of GFRP laminates coupled to stainless steel anchorage system in order to avoid corrosion phenomena. The FRP type should be selected appropriately to assure high durability in sea environment.

Scaled reinforced masonry house retrofitted using FRP was experimentally investigated in [5]. This intervention is provided to improve structural efficiency under intense ground motion. Without any reinforcement, shaking table tests have proven that even small input motions cause fatal damages or total collapse of the masonry house. The FRPs, which were arranged in vertical direction, can significantly mitigate the damages to the house. Several specimens are tested using different reinforcement ratios. The optimum FRP reinforcement ratio depends on the structure's geometry, roof weight, brick surface and the epoxy used. It was also found that FRP can be used only on single faces of the walls, reducing the time and cost without affecting the performances. In [6], a series of static tests are performed to investigate the effectiveness of the FRP reinforcement on a full-scale masonry house. Strengthening the masonry walls with CFRP strips improves significantly both the load-bearing capacity and ultimate lateral displacement of the masonry wall.

Another inexpensive solution for masonry retrofitting is using steel wire mesh [7] or steel bands [8]. In order to drop down the retrofitting cost, bamboo sheets are even used for masonry retrofitting in a residential building as reported in [9][10].

In many literatures, several different methods are presented in modeling the FRP reinforcement. In [1], the FRP reinforcement applied on masonry church is modeled as 2D shell elements with elastic-plastic behavior in tension. The interaction between masonry and FRP strip is assumed perfectly bonded. The reinforced masonry churches were evaluated through nonlinear time history (NLTH) analyses.

In [11], to investigate the behavior of FRP reinforced-masonry wall subjected to monotonic and cyclic loading, the FRP reinforcement is modeled as 2D shell element. A meso-scale masonry model is developed with element-based cohesive element to simulate both unreinforced and FRP-strengthened masonry walls. However, the FRP is assumed to be orthotropic and is characterized by the behavior of lamina which are assumed to remain elastic. Fracture and delamination failure of the FRP are not considered.

[a] Civil Engineering Department, Institut Teknologi Sepuluh Nopember, ITS Campus, Sukolilo, Surabaya 60111, Indonesia. *Corresponding author email address: ahmad.basshofi@its.ac.id

[b] Architectures, Built Environtment, and Construction Engineering Department, Politecnico di Milano, Milano 20133, Italy.

Figure 1 A scaled unreinforced masonry house in the experimental work [16].

A numerical model was established in [12] in order to evaluate the response of out-of-plane loaded calcarenite masonry walls strengthened with vertical CFRP strips applied on the substrate by means of epoxy resin. The element type used for meshing the FRP strips was a 4-node quadrilateral shell element (S4R) with reduced integration and large-strain formulation.

On the other hand, in [13], FE analyses were carried out on a reinforced masonry wall in which the FRP is modeled as 2D truss elements with elastic-plastic behavior. The model considers the behavior of the interface between the CFRP and the masonry by considering the effect of bonding failure and bond-slip effect among contacting surfaces.

A simplified model is presented in [14] to reproduce the behavior of FRP-strengthened masonry panels. In particular, the FRP-strips are modeled as truss elements directly tied to the nodes of the mesh of the panel and characterized by a no compressive strength and an elastic-brittle behavior in tension. This modeling method aims to take into account the loss of the strengthening contribution when a complete delamination occurs in the FRP strips.

In [15], a numerical analysis on the in-plane shear capacity of tuff masonry panels externally reinforced with FRP diagonal layout was carried out. The FRP is modeled by means of truss model approach. The shear contribution of the reinforcement was computed from the FRP strip placed along the diagonal in tension, neglecting the contribution of the FRP in compression.

SCALED MASONRY HOUSE PROTOTYPE

The model of the masonry house refers to the prototype scaled to 1:3 tested in [16], see Figure 1. The thickness of the wall is 85 mm and the size of the window opening is 400x300 mm. A loading beam is used to apply a lateral loading to the masonry house. Two hollow steel beams are used to transfer four concentrated vertical loads (Pv) to generate a 0.5 MPa of vertical pressure to the masonry wall. The finite element (FE) model and the dimensions of the masonry house, which consists of about 9500 four-node tetrahedral elements, are shown in Figure 2. The size of a single element is about 80 mm. A rigid slab is placed under the house.

The non-linear behavior of masonry is modeled through the Concrete Damage Plasticity (CDP) model proposed in [17] and then extended by [18], which is available within the ABAQUS software code. Although originally conceived to describe the non-linear behavior of concrete, the model can be used for masonry through a proper adaptation of the main parameters [19]. Table 1 summarizes the values of the parameters adopted for the

CDP model, where dilatation angle is angle due to a variation in volume of the material following the application of a shear force; eccentricity is the distance between the points of intersection with the p-axis of the cone and the hyperbola in the p-q plane, where p is the hydrostatic pressure stress and q is the Mises equivalent stress; σ_{b0}/σ_{c0} is the strength ratio between the biaxial and uniaxial compression strength; K_c is the ratio between the second stress invariant on the tensile meridian and the one on the compressive meridian; and viscosity is a numerical parameter which allows to reach convergence in softening without affecting the accuracy of the results.

The stress-strain relationship in tension adopted for the dynamic analyses here presented in Figure 3 satisfies a linear-elastic branch up to the peak stress σ_{t0} = 0.19 MPa. Then, micro-cracks start to propagate within the material

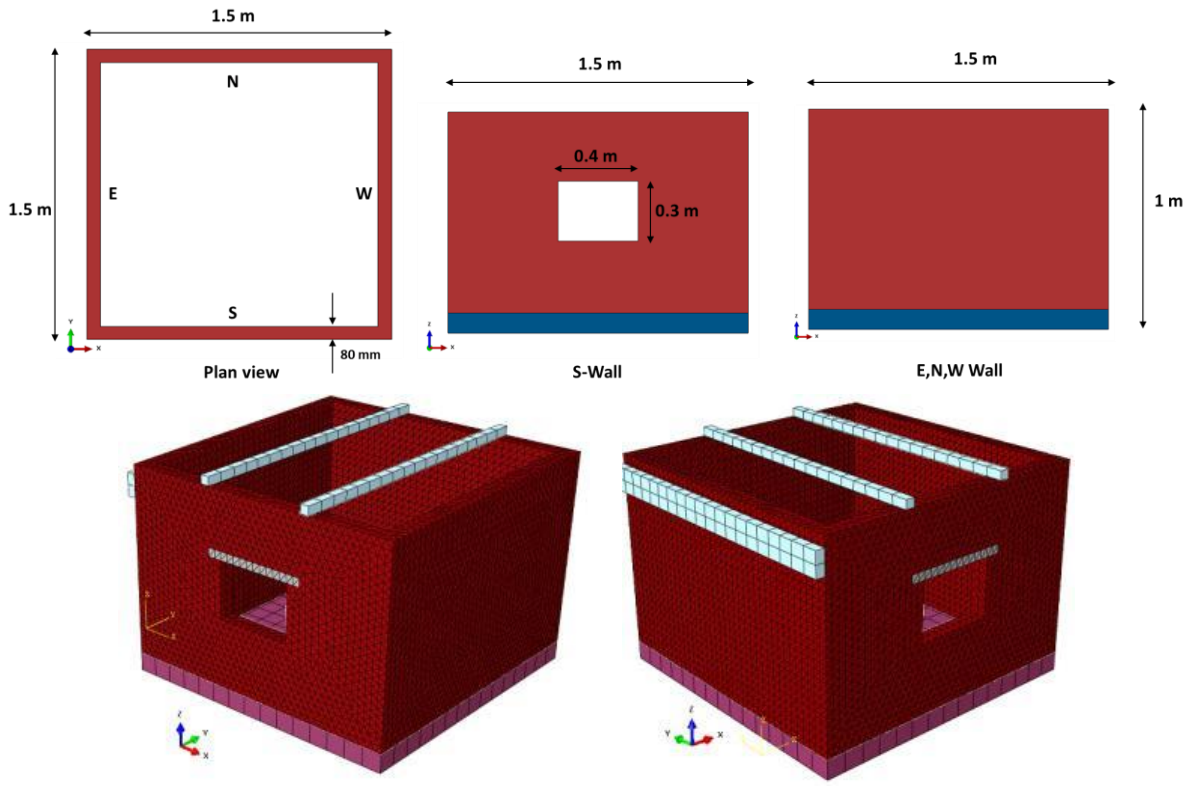

Figure 2 Dimensions and FE model of the unreinforced masonry house.

leading to a macroscopic softening. In compression, see Figure 3., the response is linear up to the yield stress σ_{c0} = 1.85 MPa. Then, a simplified linear hardening is assumed up to the crushing stress σ_{cu} 2.4 MPa, followed by a linear softening branch. The damage variables in tension (index "t") and compression (index "c") are determined by means of the following standard equations, Eq. (1) and (2), while the schematic illustration is shown in Figure 4.:

$$\sigma_t = (1 - d_t)\, E_0\, (\varepsilon_t - \varepsilon_t^{pl}) \quad (1)$$

$$\sigma_c = (1 - d_c)\, E_0\, (\varepsilon_c - \varepsilon_c^{pl}) \quad (2)$$

where σ_t, σ_c = uniaxial stresses; E_0 = initial elastic modulus; ε_t, ε_c = uniaxial total strains; ε_t^{pl}, ε_c^{pl} = equivalent plastic strains; and, d_t, d_c = damage parameters.

Table 1 Values of the parameters adopted for the CDP model for masonry

Dilatation angle	Eccentricity	σ_{b0}/σ_{c0}	K_c	Viscosity
10	0.1	1.16	0.667	0.0001

It can be figured out that the compressive strength of masonry corresponds to a combination of mortar and brick strength, while in tension, the strength of masonry is more related to the mortar one, due to its very low tensile strength. Furthermore, it should be pointed out that the global damage of a structure is likely determined by tensile and shear stresses, as the compressive loads are relatively low.

ONE-HALF CYCLIC LOADING TEST ON THE UNREINFORCED MASONRY

A one half cyclic lateral loading is applied to the house, as shown in Figure 1. The loading is performed up to a negative stiffness, followed by unloading phase. Figure 5 shows the damage of the masonry house in the experimental campaign after one-half cycle of loading. The damage mainly appears as a horizontal crack, which may indicate a sliding failure of the brick mortar interface. This type of failure may be not reproducible in the numerical modeling.

Figure 6 shows the tensile damage of the masonry in the Abaqus FE model, while the comparative displacement-force curves of the experiment and numerical model are presented in Figure 7. It can be seen that the diagonal cracks take place during the lateral loading, mainly on the two walls parallel to the loading direction. The red patterns represent the masonry elements that exhibit tensile stress close or greater to the ultimate tensile stress σ_{t0} = 0.19 MPa. More damages are observed on the wall with window opening. These are different when compared to the damages observed in the experimental, where a sliding failure of the brick mortar interface took place, see Figure 5.

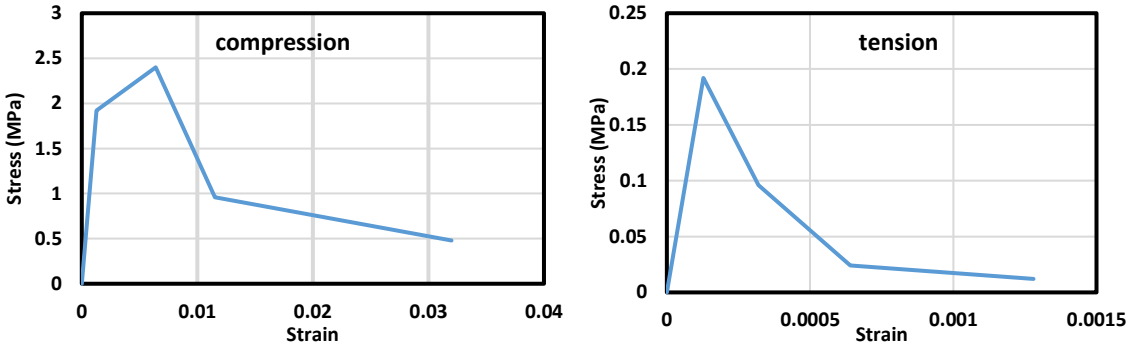

Figure 3 Strain-stress relations adopted for the simplified uniaxial behavior of masonry in compression and tension

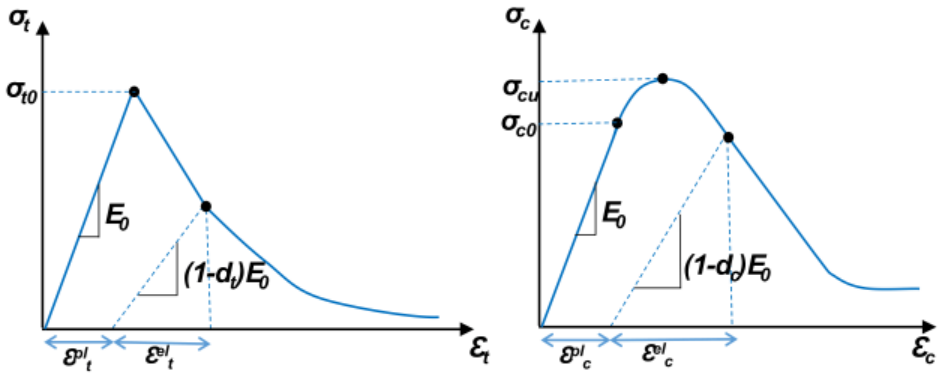

Figure 4 Schematic uniaxial behavior of masonry in compression and tension and the parameters involved

Figure 5 Damage of the unreinforced masonry house after one half cycle lateral loading in the experimental work [16].

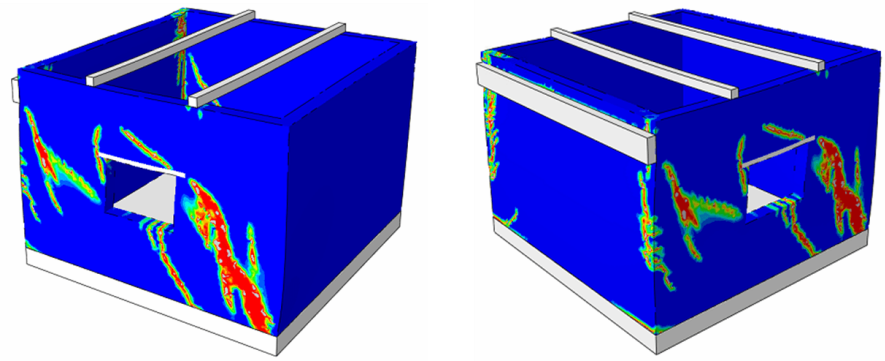

Figure 6 Tensile damages of the unreinforced masonry house in the FE model after one half cycle lateral loading.

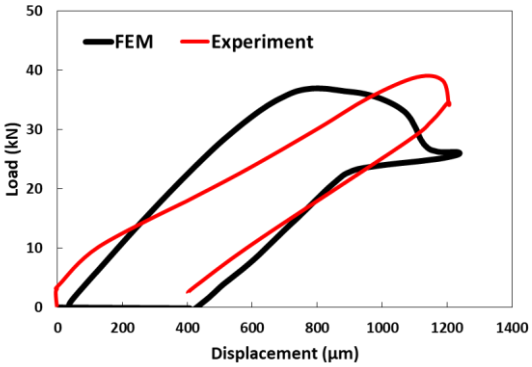

Figure 7 Lateral force-displacement of the unreinforced masonry house.

RETROFITTING USING FRP STRIP

Figure 8 shows the prototype of the masonry house retrofitted using carbon FRP (Brace BASF) strip on the side wall perpendicular to the loading direction and. The properties of the FRP are the following: Young modulus of the fiber (E_f)=230 GPa; Young modulus of the adhesive (E_a)=3500 MPa; tensile strength of the fiber=5000 MPa; tensile strength of the adhesive=35 MPa; thickness of the fiber=0.165 mm; thickness of the adhesive =0.73 mm; width of the fiber=50 mm. In addition, a roof timber diaphragm is also inserted.

The numerical model of the masonry retrofitted using FRP strip is shown in Figure 9. The FRP reinforcement consists of a single layer of FRP which is bonded to the masonry wall using adhesive. The FRP and adhesive are modeled as two separated isotropic solid materials and meshed using C3D8 elements with size about 12x12mm. Plasticity behaviors in tension as shown in Figure 10 are applied to characterize both materials. By doing so, plasticity in the adhesive material may represent the peeling of the FRP reinforcement. The constitutive model of the FRP damage-plasticity is identical to which of masonry material, as seen in Figure 4 and Equations (1) and (2).

The plasticity in compression for both materials is considered identical to which of the masonry in order to avoid convergences problem. However, as the thickness of the FRP and adhesive is thin, their contribution in compressive behavior of the global structure is negligible.

Figure 11 presents the damage patterns of the retrofitted masonry in the experimental work after the test. The diagonal cracks mainly occurred on the top corner of the masonry house and around the window opening. This reveals that sliding failure of the mortar joins, as reported in the unreinforced model in the experimental test, can be avoided by the presence of FRP reinforcement. Peeling of the FRP reinforcement was also observed in the experiment. These damage patterns are reasonably reproduced through the FE analysis, as reported in Figure 12: the cracks develop from the corner of the window opening and then propagate diagonally through the wall.

Figure 13 presents the comparative displacement-force curves after a pushover loading of the masonry house retrofitted using FRP, obtained from the experiment and FE analyses. It should be noted that in the experimental test, no unloading path was produced due to the limitation of the testing device. Thus in Figure13, only the loading curve up to 11000 μm is presented. In the FE simulations, two values of masonry ultimate tensile strength were considered, 0.2 MPa and 0.5 MPa. It is because that after the experimental testing on the unreinforced model, the specimen was restored using grouting mortar and then retrofitted using FRP. Thus, an increase of tensile strength was expected. However, as seen in Figure 13, the FE models somehow does not represent well the results of the experimental test. It may be caused buy the issue of FRP activation. In the experimental curve, the FRP seemed to contribute to the strength of the masonry house just after the yielding force of the masonry was reached. Such an issue was not taken into account in the FE models.

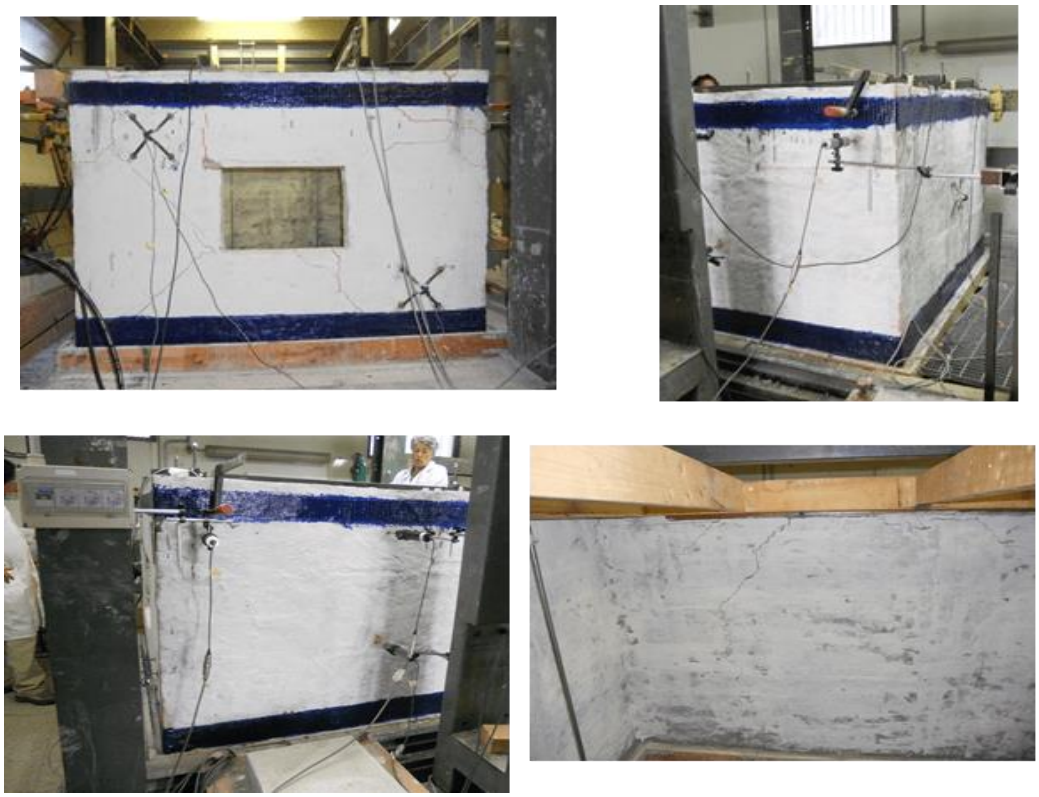

Figure 8 Prototype of the retrofitted masonry house using FRP in the experimental campaign [16].

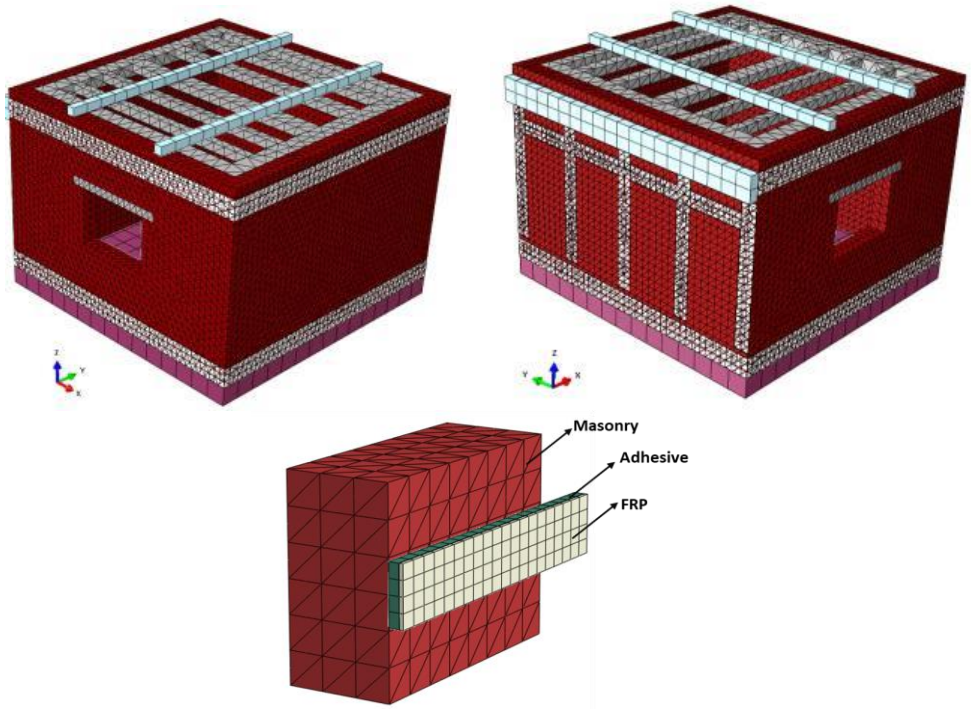

Figure 9 FE model of the retrofitted masonry house and the detail of the FRP reinforcement.

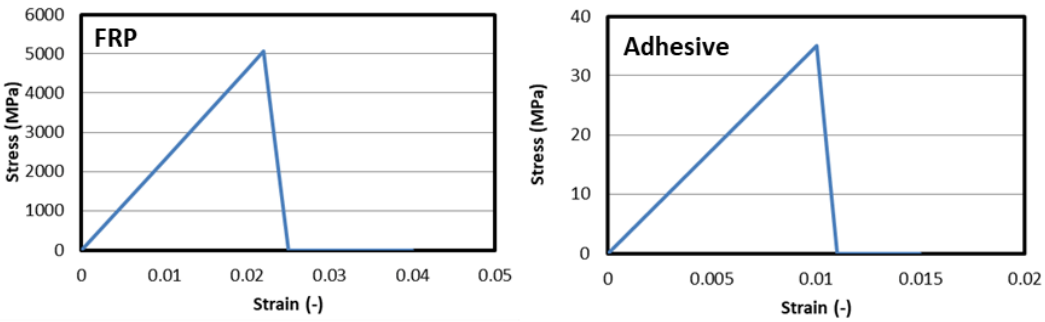

Figure 10 Simplified strain stress relation of FRP and adhesive in tension.

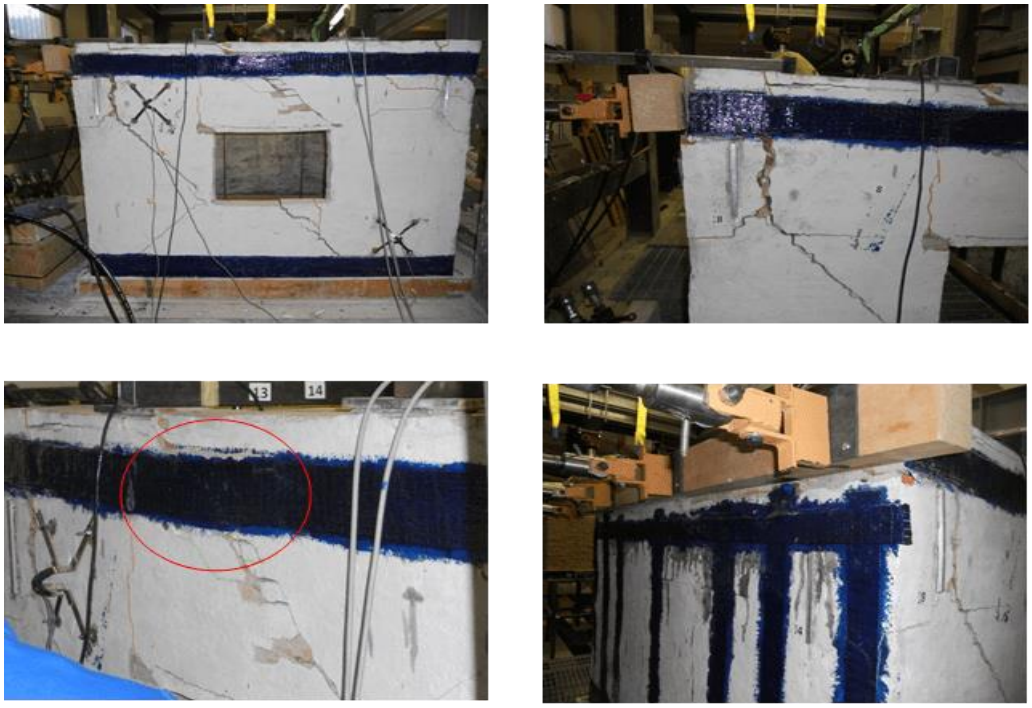

Figure 11 Damage of the retrofitted masonry house after the test [16].

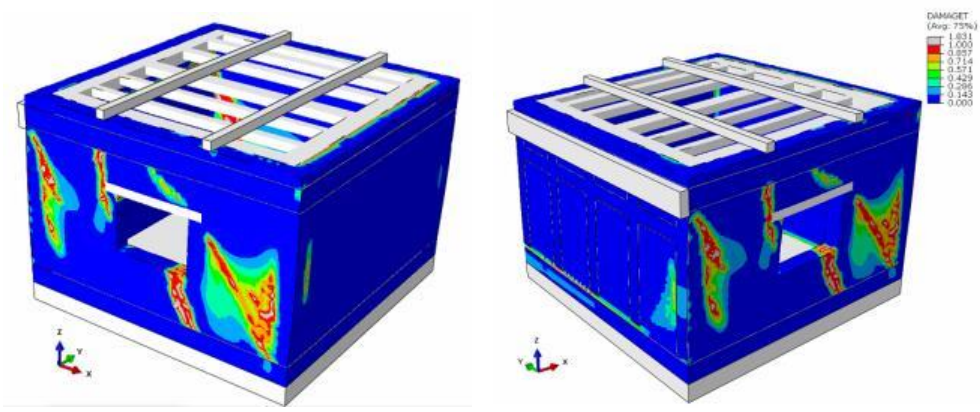

Figure 12 Tensile damage of the retrofitted masonry house in the FE model after the test.

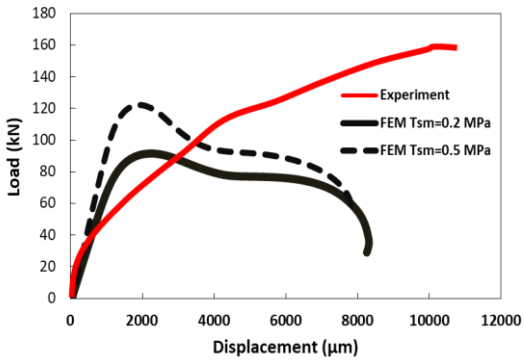

Figure 13. Lateral force-displacement of the masonry house retrofitted using FRP strip. (Tsm : ultimate tensile strength of masonry).

CONCLUSIONS

In the experimental test on the unreinforced masonry (UM) prototype, a sliding failure between masonry bricks and mortar is dominant. This type of failure may be not reproducible in the FE simulation. The ultimate lateral load of the UM prototype is about 38 kN and both experiment and FE analysis present a good agreement.

The FRP reinforcement and the adhesive are modeled as two separated solid isotropic materials and are characterized by damage-plasticity behavior. Using such a method, the plasticity in adhesive part may represent the peeling of the FRP layers.

Using the FRP reinforcement model A, in the experimental test, the damages mainly take place at the top corner of the wall and around the window opening, in accordance with the FE analysis. Meanwhile, using FRP reinforcement model A, the ultimate lateral load dramatically increases up to 160 kN, as presented in the experimental result. An improvement of the FE model of the retrofitted masonry using FRP could be done by taking into account the activation delay of the FRP reinforcement.

REFERENCES

[1] Milani, G., Shehu, R., & Valente, M. (2017). Possibilities and limitations of innovative retrofitting for masonry churches: Advanced computations on three case studies. *Construction and Building Materials*, *147*, 239-263.

[2] Bednarz, Ł. J., Jasieńko, J., Rutkowski, M., & Nowak, T. P. (2014). Strengthening and long-term monitoring of the structure of an historical church presbytery. *Engineering Structures*, *81*, 62-75.

[3] Cosenza, E., & Iervolino, I. (2007). Case study: seismic retrofitting of a medieval bell tower with FRP. *Journal of Composites for Construction*, *11*(3), 319-327.

[4] Ceroni, F., & Prota, A. (2009). Case Study: Seismic Upgrade of a Masonry Bell Tower Using Glass Fiber-Reinforced Polymer Ties. *Journal of Composites for Construction*, *13*(3), 188-197.

[5] Saleem, M. U., Numada, M., Amin, M. N., & Meguro, K. (2016). Seismic response of PP-band and FRP retrofitted house models under shake table testing. *Construction and Building Materials*, *111*, 298-316.

[6] Foraboschi, P., & Vanin, A. (2013). New methods for bonding FRP strips onto masonry structures: experimental results and analytical evaluations. *Composites: Mechanics, Computations, Applications: An International Journal*, *4*(1).

[7] Kadam, S. B., Singh, Y., & Li, B. (2014). Strengthening of unreinforced masonry using welded wire mesh and micro-concrete–behaviour under in-plane action. *Construction and Building Materials*, *54*, 247-257.

[8] Choudhury, T., Milani, G., & Kaushik, H. B. (2015). Comprehensive numerical approaches for the design and safety assessment of masonry buildings retrofitted with steel bands in developing countries: The case of India. *Construction and Building Materials*, *85*, 227-246.

[9] Puri, V., Chakrabortty, P., Anand, S., & Majumdar, S. (2017). Bamboo reinforced prefabricated wall panels for low cost housing. *Journal of Building Engineering*, *9*, 52-59.

[10] Iyer, S. (2002). *Guidelines for building bamboo-reinforced masonry in earthquake-prone areas in India* (Doctoral dissertation, University Of Southern California).

[11] Zhang, S., Yang, D., Sheng, Y., Garrity, S. W., & Xu, L. (2017). Numerical modelling of FRP-reinforced masonry walls under in-plane seismic loading. *Construction and Building Materials*, *134*, 649-663.

[12] Monaco, A., Minafò, G., Cucchiara, C., D'Anna, J., & La Mendola, L. (2017). Finite element analysis of the out-of-plane behavior of FRP strengthened masonry panels. *Composites Part B: Engineering*, *115*, 188-202.

[13] Batikha, M., & Alkam, F. (2015). The effect of mechanical properties of masonry on the behavior of FRP-strengthened masonry-infilled RC frame under cyclic load. *Composite Structures*, *134*, 513-522.

[14] Grande, E., Imbimbo, M., & Sacco, E. (2013). Finite element analysis of masonry panels strengthened with FRPs. *Composites Part B: Engineering*, *45*(1), 1296-1309.

[15] Marcari, G., Oliveira, D. V., Fabbrocino, G., & Lourenço, P. B. (2011). Shear capacity assessment of tuff panels strengthened with FRP diagonal layout. *Composites Part B: Engineering*, *42*(7), 1956-1965.

[16] Indirli M., Bati S.B., Tralli A.M. Verifica sperimentale del dispositivo in SMA in serie con rinforzi in FRP: prove preliminari. ENEA Report 2011.

[17] Lubliner J, Oliver J, Oller S, Oñate E. A plastic-damage model for concrete (1989). International Journal of Solids and Structures 1989;25:299-326.
[18] Lee J, Fenves GL. Plastic-Damage Model for Cyclic Loading of Concrete Structures (1998). Journal of Engineering Mechanics 1998;124:892-900.
[19] Valente M, Milani G. Damage assessment and collapse investigation of three historical masonry palaces under seismic actions. Engineering Failure Analysis 2019;98:10-37.
[20] Valente M, Barbieri G, Biolzi L. Seismic assessment of two masonry Baroque churches damaged by the 2012 Emilia earthquake. Engineering Failure Analysis 2017;79:773-802.
[21] Toopchi-Nezhad, H., Tait, M. J., & Drysdale, R. G. (2009). Shake table study on an ordinary low-rise building seismically isolated with SU-FREIs (stable unbonded-fiber reinforced elastomeric isolators). Earthquake Engineering & Structural Dynamics, 38(11), 1335-1357.